



# Hydroxyl radical-mediated degradation of salicylic acid and methyl paraben: an experimental and computational approach to assess the reaction mechanisms

Evrım Arslan<sup>1</sup> · Basak Savun Hekimoglu<sup>2</sup> · Sesil Agocan Cinar<sup>1</sup> · Nilsun Ince<sup>2</sup> · Viktorya Aviyente<sup>1</sup>

Received: 24 April 2019 / Accepted: 22 July 2019 / Published online: 13 September 2019  
© Springer-Verlag GmbH Germany, part of Springer Nature 2019

## Abstract

Advanced oxidation processes (AOPs) using various energy sources and oxidants to produce reactive oxygen species are widely used for the destruction of recalcitrant water contaminants. The current study is about the degradation of two emerging pollutants—salicylic acid (SA) and methyl paraben (MP)—by high-frequency ultrasonication followed by identification of the oxidation byproducts and modeling of the reaction mechanisms using the density functional theory (DFT). The study also encompasses prediction of the aquatic toxicity and potential risk of the identified byproducts to some aquatic organisms using the ECOSAR (Ecological Structure Activity Relationships) protocol. It was found that the degradation of both compounds was governed by  $\bullet\text{OH}$  attack and the pathways consisted of a cascade of reactions. The rate determining steps were decarboxylation ( $\sim 60 \text{ kcal mol}^{-1}$ ) and bond breakage reactions ( $\sim 80 \text{ kcal mol}^{-1}$ ), which were triggered by the stability of the reaction byproducts and overcome by the applied reaction conditions. Estimated values of the acute toxicities showed that only few of the byproducts were harmful to aquatic organisms, implying the environmental friendliness of the experimental method.

**Keywords** PPCPs ·  $\bullet\text{OH}$  · DFT · Sonolysis · Reaction mechanism · AOPs · ECOSAR

## Introduction

Pharmaceuticals and personal care products (PPCPs) are extensively used in daily life via their presence in human and veterinary medicine, cosmetics, and numerous food products. Inevitably, they are readily discharged to sewage treatment facilities, which they usually bypass and find their way to the aquatic environment with the effluent of the treatment

system (Wales et al. 2008; Savun-Hekimoğlu and Ince 2019). The presence of PPCPs in water is a global environmental concern due to their recognition with aquatic toxicity and potential threat to human health (Brodin et al. 2013).

Advanced oxidation processes (AOPs), which are capable of in situ  $\bullet\text{OH}$  generation, have lately received considerable attention in water treatment, owing to the high reactivity and non-selectivity of the OH radical, and the sludge-free character of the process (Gültekin and Ince 2007). The most common methods of AOPs are UV/ $\text{H}_2\text{O}_2$ , ozonation, electromagnetic radiation,  $\text{TiO}_2$ -photocatalysis,  $\gamma$ -irradiation, and ultrasonication (Ince, 2018). In all AOPs, the attack of  $\bullet\text{OH}$  to organic molecules is initiated either by H-abstraction or direct addition, both of which lead to the formation of lower molecular weight and less toxic intermediates.

Ultrasonic irradiation of water leads to high-energy chemistry via the formation of extreme temperatures and pressures upon the implosion of acoustic cavitation bubbles containing dissolved gases and water vapor (Suslick et al. 1986). Temperatures and pressures during the implosion process are as high as 5000 K and 2000 atm, at which water molecules and the entrapped gases undergo thermal fragmentation to

Responsible editor: Vítor Pais Vilar

**Electronic supplementary material** The online version of this article (<https://doi.org/10.1007/s11356-019-06048-3>) contains supplementary material, which is available to authorized users.

✉ Nilsun Ince  
ince@boun.edu.tr

✉ Viktorya Aviyente  
aviye@boun.edu.tr

<sup>1</sup> Department of Chemistry, Boğaziçi University, Bebek, 34342 Istanbul, Turkey

<sup>2</sup> Institute of Environmental Sciences, Boğaziçi University, Bebek, 34342 Istanbul, Turkey

yield a variety of radical species. Under these conditions, intense mechanical, chemical, and thermal effects are observed (Mason and Peters 2002). Hence, the use of ultrasound in AOPs is based on the formation of OH radicals upon pyrolytic decomposition of water molecules during the collapse of cavity bubbles. It has been established that if sonication is applied at low frequencies, mechanical effects of ultrasound dominate, whereas at high frequencies chemical effects are more important. Although the full mechanism has not been so far elucidated, it is accepted that low frequencies (20–80 kHz) preferentially lead to mechanical and physical effects, while high frequencies (150–2000 kHz) favor the production of more HO radicals, leading to more intense chemical effects (Mason et al. 1992). The attractiveness of sonochemistry in AOPs arise from the fact that no chemicals are required to produce radical species, and no waste sludge is produced as a byproduct of the process. Nevertheless, the challenge remains, as the energetic and financial competitiveness of the method to the existing processes performed in silent conditions are still under investigation (Chatel et al. 2016).

Salicylic acid (SA) and its derivatives constitute a group of PPCPs that are commonly used in analgesics and antipyretics, and are available in a wide variety of formulations. Overdosing of the compound has been reported as toxic (Nakada et al. 2007) leading to symptoms such as headache and nausea (Chaniotakis et al. 1989). SA is frequently detected in water and wastewater systems at relatively high concentrations, indicating the necessity to eliminate it before the water is reclaimed and transferred to distribution systems (Taylor and Stamatis n.d.). Published studies related to sonochemical degradation of SA have shown that the compound is highly reactive with OH radicals to readily yield dihydroxybenzoic acid, followed by the production of smaller aromatic compounds (Amin et al. 2010). Note also that salicylic acid is commonly used as a model compound to monitor the formation of hydroxyl radicals in advanced oxidation or other chemical reactions (Karnik et al. 2007).

Parabens are another group of PPCPs that are widely used in toothpaste, cosmetics, textiles, foodstuff, and beverages, owing to their preservative and antibacterial properties (Savun-Hekimoğlu and Ince 2017). It has been reported that annually, 8000 tons of parabens are produced and a large fraction of them are introduced into the aquatic system via excretion and waste discharge (Ramaswamy et al. 2011). Among all, methyl paraben (MP) is the most highly consumed paraben and is classified under “emerging contaminants” not only because of its aquatic toxicity, but also due to its potential contribution to the incidence of breast cancer (Márquez-sillero et al. 2010). The literature on sonochemical decomposition of MP at high-frequency ultrasound is limited to a few studies focusing on optimization of the operational parameters and integration of the method with clay minerals (Savun-Hekimoğlu and Ince 2019) and investigation of the driving

mechanisms as hydroxylation and hydrolysis (Sasi et al. 2015). The latter research has also reported complete mineralization of the compound as the evidence of the high efficiency of sonochemistry compared with all other AOPs.

The purpose of this study was to investigate the degradability of SA and MP by high-frequency ultrasound to elucidate the reaction kinetics and to propose reaction mechanisms that support the experimental results. Additionally, the study covers the prediction of the aquatic toxicity of the parent and oxidation byproducts at three test levels to test the environmental safety of the ultrasonic method as an AOP.

## Materials and methods

Salicylic acid and methyl paraben were purchased from Sigma-Aldrich (>99% purity) and used without further purification. HPLC-grade acetonitrile and phosphoric acid were purchased from Merck (Istanbul) for use in the analysis of the compounds during sonication.

## Experimental

The ultrasonic reactor was a multi-frequency plate-type with a 500-ml glass cell and a 120-W generator, connected to three piezoelectric transducers (22 cm<sup>2</sup>) emitting individually at 572, 861, and 1164 kHz (Ultraschall-Meinhardt, Germany). The effective volume and power density in the reactor were 250 mL and 0.21 W mL<sup>-1</sup>, the latter estimated by calorimetric measurements. Initial solute concentrations and reaction time were 10 mg L<sup>-1</sup> and 30 min, respectively. Test samples of 10 mg L<sup>-1</sup> adjusted to pH 3.0 were exposed to 572 kHz ultrasound for 30 min, during which samples were collected periodically for the analysis of target compound concentrations and total organic carbon (TOC). Samples were also withdrawn at  $t = 10$  min for use in the detection and identification of the oxidation byproducts.

## Analytical

Concentrations of SA and MP were determined by a Shimadzu LC-20AT HPLC with a 20A UV-Vis photo diode array detector, an Inertsil ODS-3 V (C18) (Hypersil BDS), and a 250 mm × 4.6 mm column. The mobile phase for SA analysis was 20 mM phosphoric acid and acetonitrile at a ratio of 50:50 (by v), and that for MP was water/acetonitrile/phosphoric acid at a ratio of 70:30:0.15. The degree of carbon mineralization was assessed by TOC analysis using a Shimadzu TOC-V CSH analyzer. The oxidation byproducts present in solution after 10-min sonolysis were identified by AB SCIEX QTRAP® 4500 LC-MS/MS system with a Turbo V™ ion source and electron spray ionization (ESI), operated at the negative and “multiple reaction monitoring” mode to

enable identification of the chemical structures. The 100-fold diluted samples were analyzed by direct infusion into the ESI source via a syringe pump at a flow rate of 10  $\mu\text{L}/\text{min}$ . Enhanced mass scanning (EMS) and enhanced product ion (EPI) scan modes were used to acquire information on parent compounds and their fragmentation patterns, respectively. The mass spectrometer was operated under the following conditions: ion source temperature, 500  $^{\circ}\text{C}$ ; curtain gas, 20 psi; nebulizer gas, 40 psi; heater gas, 60 psi; CAD gas, low; IS pos, + 5500 V. The EMS spectra of the samples were obtained by scanning over the  $m/z$  range 55–155 at a rate of 10000 Da/s, a collision energy of 10 V and a decluttering potential of 70 V. All data were acquired and processed using the Analyst 1.6.2. Software.

## Computational

The reaction of SA and MP with the medium ( $\bullet\text{OH}$ ,  $\text{H}_2\text{O}$ ) was considered by using the basic principles of organic chemistry such as  $\bullet\text{OH}$  addition, H abstraction, water elimination, bond rupture, and aromatization with a goal of rationalizing the formation of the experimentally observed byproducts. The proposed mechanisms were modeled using the density functional theory (DFT), the B3LYP functional and the 6–31 + G(d) basis sets (Lee et al. 1988), (Becke 1993a), (Becke 1993b). A conformational search around single bonds was performed for the structures corresponding to local minima, the energetics discussed in the results are based on the global minima. Transition state structures were characterized by a single imaginary frequency. All the quantum chemical calculations were performed using Gaussian 09 software package (Frisch et al. 2009). The reactions were conducted in water ( $\epsilon = 78.36$ ) environment using the integral equation formalism polarizable continuum model (IEF-PCM) at 298K. The intrinsic reaction coordinate (IRC) calculations were held to prove that each transition state is connected to the corresponding reactants (RC) and products (PC). The acute toxicities of SA, MP, and their oxidation byproducts to green algae, daphnia, and fish were estimated in terms of maximum effective ( $\text{EC}_{50}$ ) and lethal ( $\text{LC}_{50}$ ) concentration using the Ecological Structure Activity Relationships software (ECOSAR 2014).

## Results and discussion

### Experimental

Normalized concentrations of SA and MP during 30-min sonolysis at 572 kHz are plotted in Fig. 1. The fitted curves ( $R^2 = 0.98$ ) show that the rate of reaction in both cases was pseudo first order, with rate constants of 0.067 and 0.091  $\text{min}^{-1}$  for SA and MP, respectively. The inset at the top of the figure shows the degree of C-mineralization

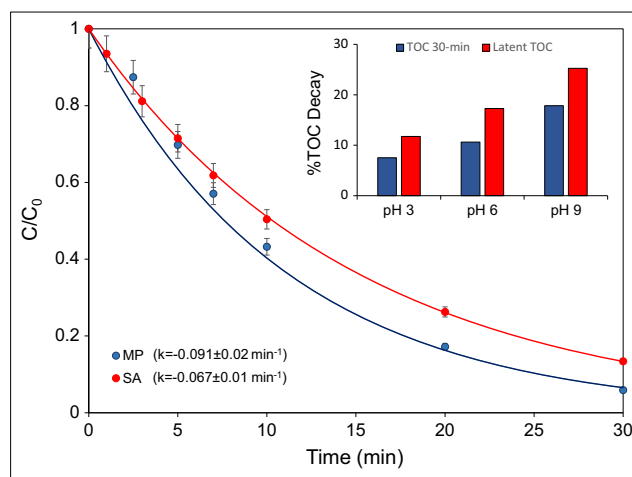


**Fig. 1** Normalized plots of concentration-time showing the rate of sonochemical degradation of SA and MP ( $C_0 = 10 \text{ mg L}^{-1}$ ) at pH 3.0. The bar chart at the right bottom shows the corresponding C-mineralization

after 30-min sonolysis and that after a 24-h silent maintenance in the dark. It was interesting to find that the mineralization process continued for a long time after the ultrasonic generator was shut down, as the indication of “latent cavitation,” i.e., the effect of stable ROS such as  $\text{H}_2\text{O}_2$  that form upon the violent collapse of acoustic cavitation bubbles.

LC/MS/MS spectra of 10-min sonicated samples of SA and MP are presented in Fig. 2a and b, respectively. For SA, we detected four major peaks at molecular weights of 62, 108, 110, and 154  $\text{g mol}^{-1}$  with intensities of 2.44, 1.53, 1.36, and 1.83, respectively. For MP, we found six major peaks at molecular weights of 85, 108, 110, 134, 138, and 150  $\text{g mol}^{-1}$  and intensities of 1.42, 0.30, 0.15, 0.50, 0.42, and 0.15, respectively. The results for SA are consistent with those of Scheck and Frimmel, who identified benzoquinone (MW = 108) and dihydroxybenzoic acid (MW = 154) as the byproducts of UV/peroxide/ $\text{O}_2$  process (Scheck and Frimmel 1995). The latter was also reported by Chang et al., together with catechol (MW = 110) as the byproducts of SA oxidation in a Fenton process (Chang et al. 2008). In another study by Guinea et al., using electrochemical oxidation techniques, dihydroxybenzoic acid, maleic acid (MW = 116), fumaric acid (MW = 116), and malic acid (MW = 134) were identified as the byproducts of SA degradation (Guinea et al. 2008).

A photocatalytic study of MP by Lin et al. with  $\text{TiO}_2$  has shown that the intermediate products were dihydroxybenzene (MW = 110), 4-hydroxybenzoic acid (MW = 138), tartaric acid (MW = 150), and benzoquinone (MW = 108), which are consistent with our findings (Lin et al. 2009). Another study done by Gmurek et al. focused on the degradation of hazardous water

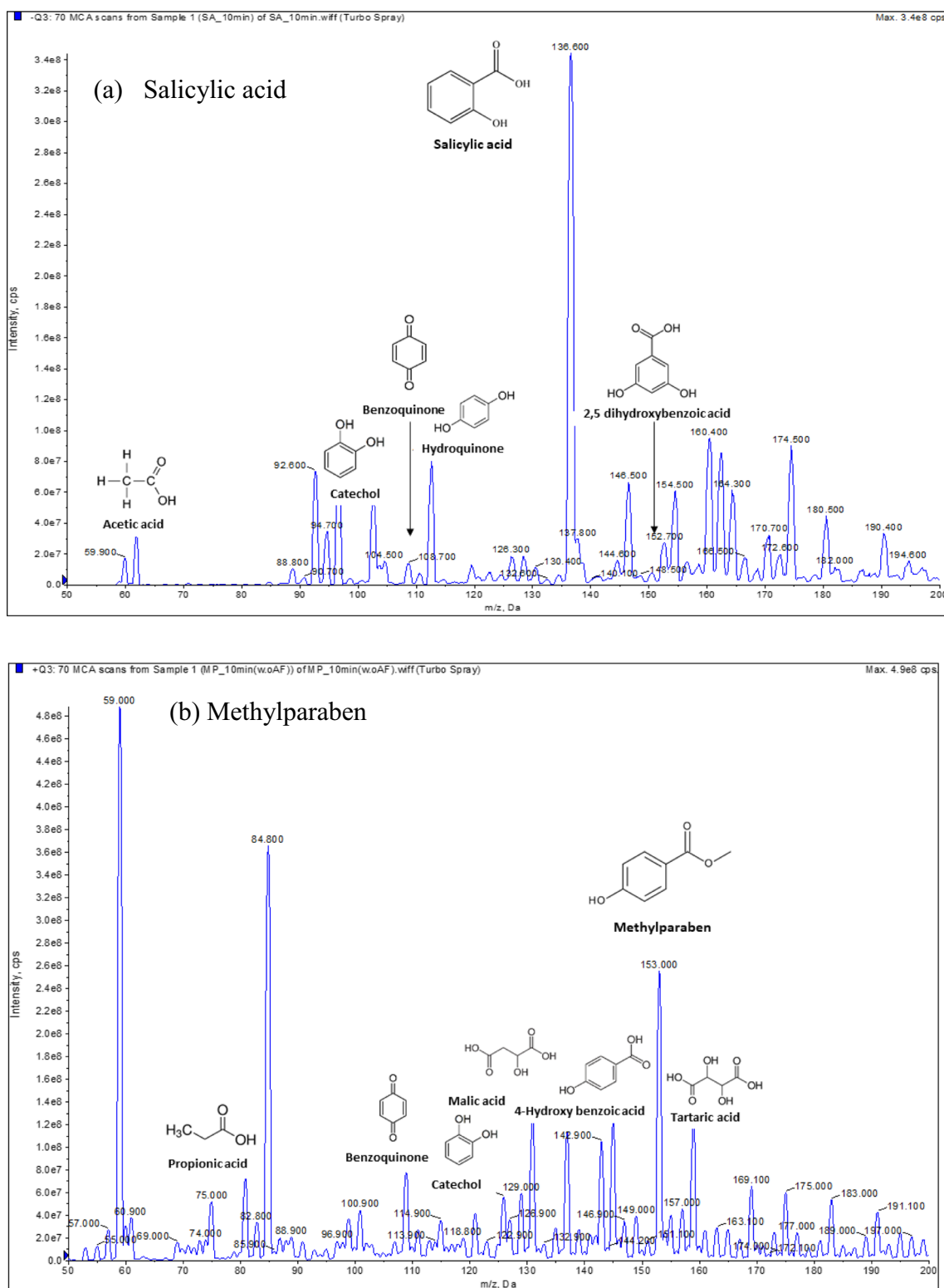


**Fig. 2** LC/MS/MS spectra of 10-min sonicated samples of SA **a** and MP **b** and structures of their identified byproducts

contaminants: methyl-, ethyl-, propyl-, butyl-, and benzylparaben using ultraviolet C lamps in the absence and presence of  $H_2O_2$  (Gmurek et al. 2015). From the byproduct analysis, it was concluded that the main

degradation products were p-hydroxybenzoic acid (MW = 138); 2,4 dihydroxybenzoic acid (MW = 154); and 3,4 dihydroxybenzoic acid (MW = 154). These experimental results are consistent with our results.

## Computational

### Salicylic acid

The energetics for the degradation mechanism of SA can be monitored step by step in Figs. 3 and 4. The potential energy surfaces of the degradation pathway of SA are displayed in Figs. S1, S2, S3, and S4. The 3D structures of the transition structures are shown in Fig. S5.

SA is primarily attacked by •OH at the ortho/para positions of the OH since these are favorable positions for the ortho/para director OH group and the meta director

carbonyl group which are already present on the ring. The ortho and para positions to •OH are attacked with very low barriers of 4.3 kcal·mol<sup>-1</sup> and 6.3 kcal·mol<sup>-1</sup>; the reaction is exothermic by 6.0 kcal·mol<sup>-1</sup> (SA6) and 3.2 kcal·mol<sup>-1</sup> (SA1) respectively. It is very likely that SA1 is attacked barrierless by another •OH to form the neutral product SA2 with very high exothermicity ( $\Delta G_{\text{rxn}} = -60.1$  kcal·mol<sup>-1</sup>). At this stage, water elimination (TS-(SA2-SA3)) is very costly ( $\Delta G^\ddagger = 41.8$  kcal·mol<sup>-1</sup>) to yield the stable product SA3 ( $\Delta G_{\text{rxn}} = -95.9$  kcal·mol<sup>-1</sup>), which is detected experimentally (MW = 154). SA8, the isomer of SA3 is formed via similar steps. We

**Fig. 3** Gibbs-free energies (kcal·mol<sup>-1</sup>) for the degradation pathway of SA into SA5 and SA10 (B3LYP/6-31 + G\*, in water)

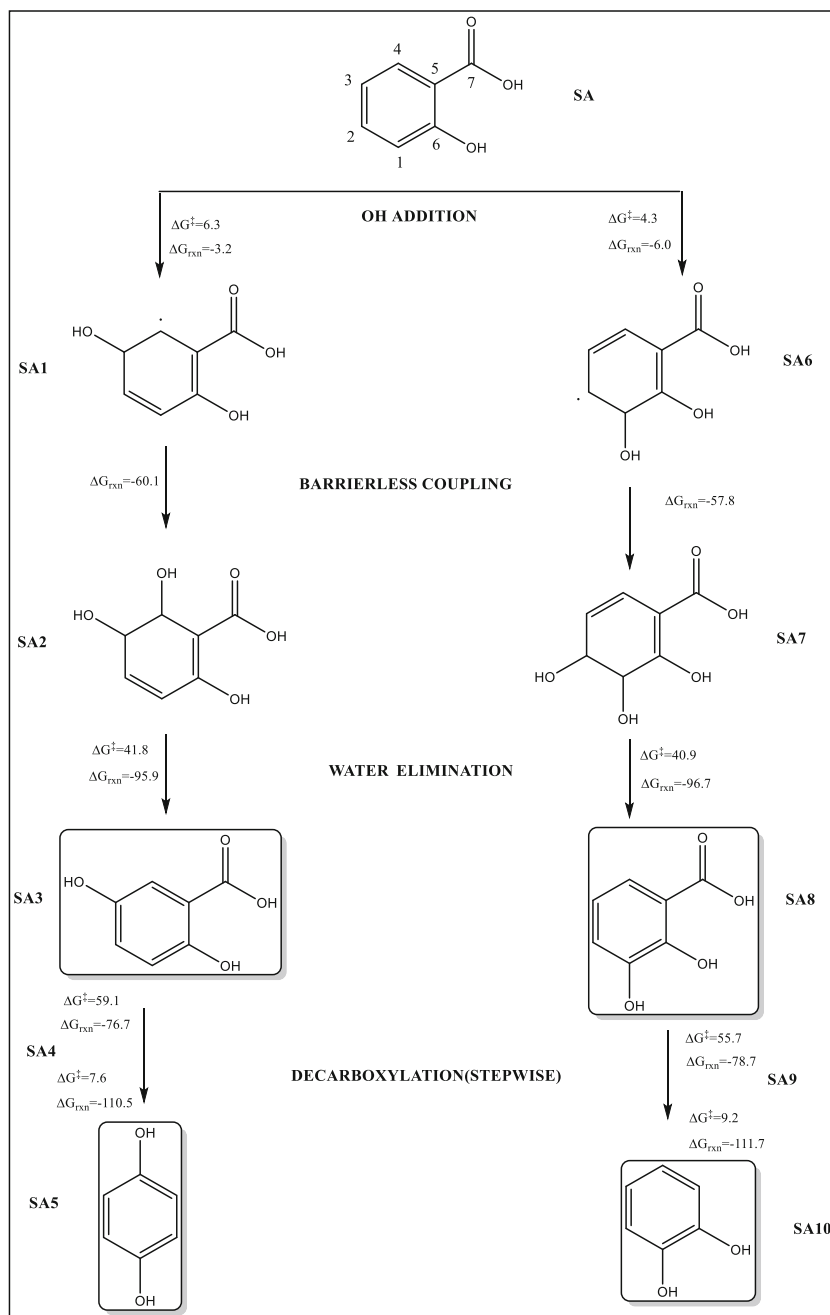
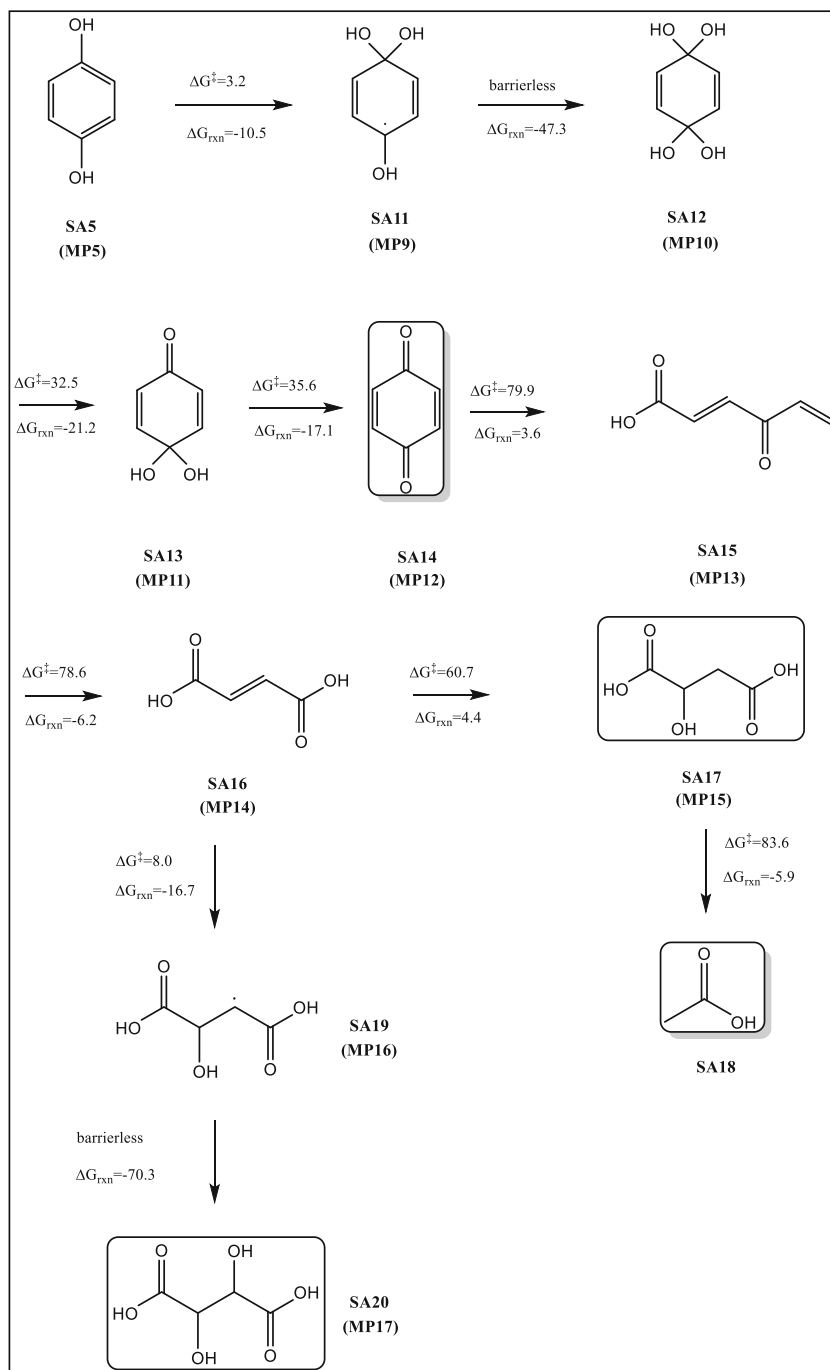


**Fig. 4** Gibbs-free energies ( $\text{kcal}\cdot\text{mol}^{-1}$ ) for the degradation pathway of SA5 into SA18 (B3LYP/6-31 + G\*, in water)



suggest the other isolated intermediate SA5 (MW = 110) to be formed in a stepwise manner, first a hydrogen shift from position 6 to position 5 forming SA4 and then decarboxylation. The driving force for this last reaction would be the high stability of the final product SA5 ( $\Delta G_{\text{rxn}} = -110.5 \text{ kcal}\cdot\text{mol}^{-1}$ ). Overall, the stabilities of the intermediates SA3 (MW = 154) and 1,4-benzenediol/hydroxyquinone (SA5, MW = 110) trigger their formation. Note that SA8 yields 1,2-benzenediol/ catechol (SA10, MW = 110) similarly along exothermic reactions. The

formation of SA10 (MW = 110) follows the same pattern as SA5.

The formation of 1,4-benzoquinone (MW = 108) can be visualized in Fig. 4 as a continuation of Fig. 3. In this mechanism, 1,4-benzenediol (SA5) gains easily 2  $\cdot\text{OH}$  groups sequentially to form the very stable species SA12 ( $-47.3 \text{ kcal}\cdot\text{mol}^{-1}$ ). SA12 yields SA14, namely 1,4-benzoquinone (MW = 108) after two consecutive  $\text{H}_2\text{O}$  eliminations. Further reactions to form the intermediate with MW = 126 involves bond rupture (TS-(SA14-SA15)) which is highly

energetic ( $79.9 \text{ kcal}\cdot\text{mol}^{-1}$ ) to yield the product SA15 ( $3.5 \text{ kcal}\cdot\text{mol}^{-1}$ ). SA15 undergoes another bond breakage with a barrier of  $78.6 \text{ kcal}\cdot\text{mol}^{-1}$  to yield SA16 ( $-6.2 \text{ kcal}\cdot\text{mol}^{-1}$ ) that abstracts  $\text{H}_2\text{O}$  to yield SA17 (MW = 108), ( $4.6 \text{ kcal}\cdot\text{mol}^{-1}$ ). SA17 can undergo bond rupture to form SA18 (MW = 60) which was detected experimentally ( $-5.9 \text{ kcal}\cdot\text{mol}^{-1}$ ).

Overall, reaction profiles yielding the experimentally detected intermediates (SA18 (MW = 60), SA14 (MW = 108), SA5 and SA10 (MW = 110), SA3 and SA8 (MW = 154)) have been suggested. Although Gibbs-free energies of activation yielding the desired intermediates are high, the products are stable, the reactions are thermodynamically driven.

### Methyl paraben

Over the past years, many varieties of AOPs (ozonation (George et al. 2014), photocatalysis (Lam et al. 2013), and electrochemical oxidation UV-irradiation (Sánchez-Martín et al. 2013)) have been extensively used for the degradation of MP, based on the power and non-selectivity of  $\bullet\text{OH}$  in oxidizing organic molecules. Many of these studies, however, have focused mainly on setting the optimum experimental conditions, disregarding the reaction mechanism (Lam et al. 2013; Sánchez-Martín et al. 2013; Tay et al. 2010). There are some studies reporting the attack of the  $\bullet\text{OH}$  to both the benzene ring and the alkyl chain, based on the identified intermediates (Lin et al. 2009; George et al. 2014). However, the specific degradation route for MP is still unclear. In a study by Gao et al., all possible degradation pathways of MP were elucidated by quantum chemical calculations and the toxicity of all intermediates was estimated (Gao et al. 2016). However, to the best of our knowledge, there are no computational studies reporting the intermediates formed by bond rupture mechanisms.

Figures 4 and 5 show the proposed mechanisms in this work for the degradation of MP. All the potential energy surfaces related to the degradation pathway of MP are displayed in Figs. S6, S7, S8, and S9. The energetics have been calculated based on the stoichiometrically balanced reactions. In water, MP (MW = 150) may undergo hydrolysis yielding MP1 with a barrier  $59.8 \text{ kcal}\cdot\text{mol}^{-1}$  and the reaction is endothermic by  $2.0 \text{ kcal mol}$ . Note that the latter intermediate MP1 (MW = 138) was also detected experimentally (Fig. 2). The reaction is followed by decarboxylation to obtain MP2 ( $-12.1 \text{ kcal}\cdot\text{mol}^{-1}$ ). Then, MP2 (MW = 94) is attacked by  $\bullet\text{OH}$ , with addition to the *o*- and *para* *p*- positions yielding MP3 (MW = 112) and MP6 (MW = 112) with low barriers and high exothermicities ( $\Delta G^\ddagger = 4.8 \text{ kcal}\cdot\text{mol}^{-1}$  and  $5.6 \text{ kcal}\cdot\text{mol}^{-1}$ ;  $\Delta G_{\text{rxn}} = -16.6 \text{ kcal}\cdot\text{mol}^{-1}$  and  $-17.9 \text{ kcal}\cdot\text{mol}^{-1}$ , respectively). It is very probable that MP3 and MP6 are attacked barrierless by another  $\bullet\text{OH}$  to form the neutral species MP4 (MW = 128,  $-65.7 \text{ kcal}\cdot\text{mol}^{-1}$ ) and MP7 (MW = 128, -

$69.2 \text{ kcal}\cdot\text{mol}^{-1}$ ). At this stage, elimination of water (TS-(MP4-MP5) and TS-(MP7-MP8)) is costly ( $34.2 \text{ kcal}\cdot\text{mol}^{-1}$  and  $40.8 \text{ kcal}\cdot\text{mol}^{-1}$ , respectively) to yield exothermically MP5 (MW = 110) and MP8 (MW = 110); the latter stable intermediates have also been detected experimentally. Note that MP5 and MP8 are identical to SA5 and SA10 respectively, thus the reactions of the degradation byproducts will be similar to those of SA5 and SA10, as discussed in the previous section.

The mechanism proposed above illustrates that  $\bullet\text{OH}$ -addition is the governing route in the degradation of MP, as also reported in the literature (Agopcan Cinar et al. 2017) for shorter alkyl chain parabens. Gao et al. (2016) have investigated the effect of alkyl chain length on the degradation mechanism of parabens and found that  $\bullet\text{OH}$ -addition was the more dominant route for the degradation of shorter parabens, such as MP. The same authors have also demonstrated the dominance of  $\bullet\text{OH}$ -addition over H-abstraction for the degradation of diclofenac (Agopcan Cinar et al. 2017).

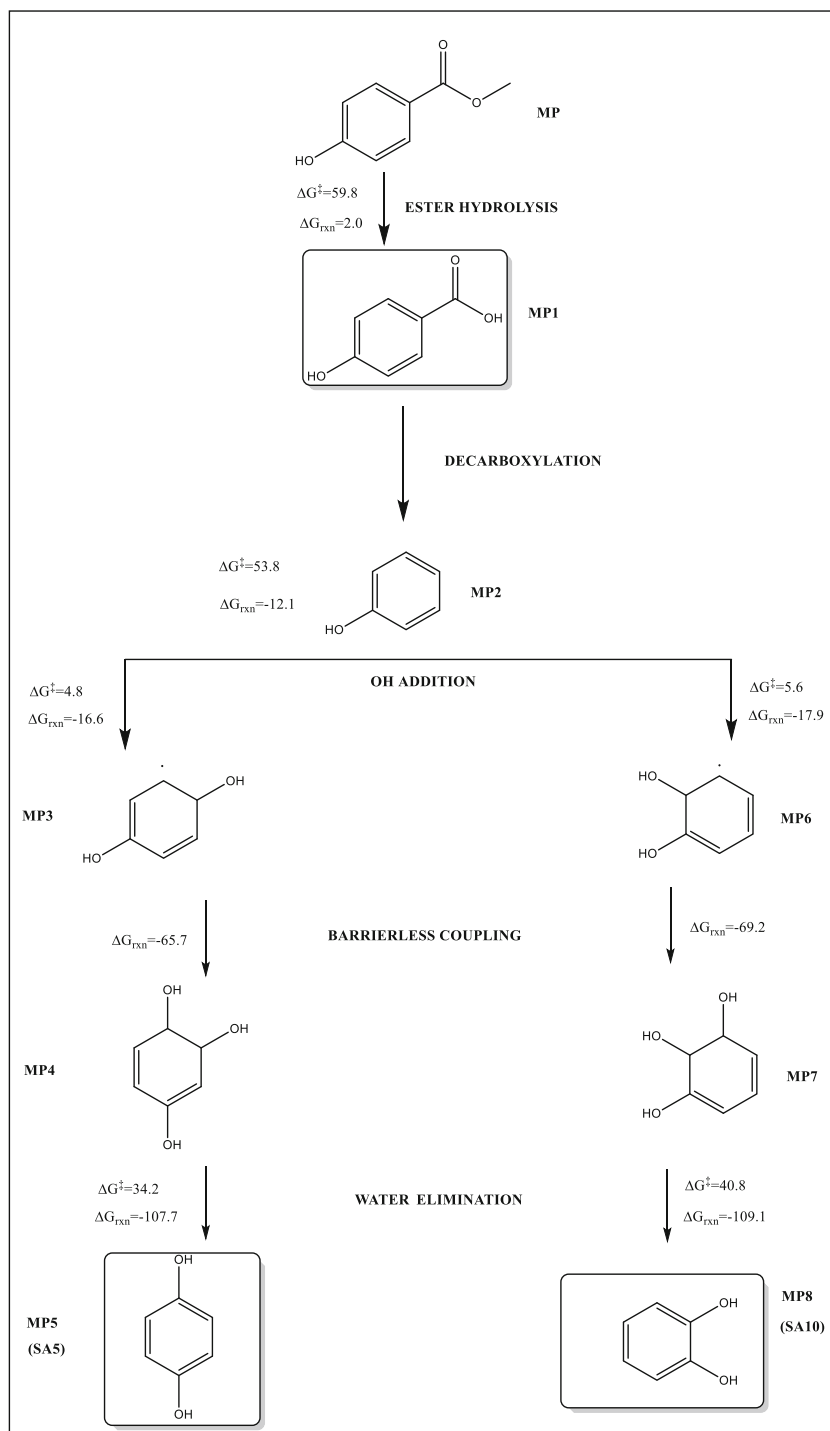
As mentioned in “**Experimental**,” the intermediate products of oxidation detected by Lin et al. (2009) for the degradation of MP are consistent with our results, i.e., dihydroxybenzene (MW = 110), 4-hydroxybenzoic acid (MW = 138), tartaric acid (MW = 150), and benzoquinone (MW = 108).

### Summary of computational findings

The pathways show the degradation of SA to acetic acid (SA18) to occur along a cascade of reactions (Figs. 3 and 4). The transformation of SA to hydroxyquinone (SA5) and catechol (SA10) have rate determining steps along the conversion of SA3 to hydroxyquinone (SA5) and SA8 to catechol (SA10). The high-energy barriers of  $59.1 \text{ kcal mol}^{-1}$  and  $55.7 \text{ kcal mol}^{-1}$  can be attributed to the decarboxylation reaction in each case. The degradation of hydroxyquinone (SA5) to acetic acid (SA18) proceeds via sequential reactions:  $\bullet\text{OH}$  addition and water eliminations followed by a highly energetic ring rupture ( $79.9 \text{ kcal mol}^{-1}$ ) to SA15. The latter undergoes C–C bond rupture ( $78.6 \text{ kcal mol}^{-1}$ ) and water addition ( $60.7 \text{ kcal mol}^{-1}$ ) to yield SA17, which finally overcomes an energetically demanding barrier ( $83.6 \text{ kcal mol}^{-1}$ ) to yield acetic acid (SA18).

The degradation pathways of methyl paraben (MP) resemble closely those of salicylic acid (SA) (Figs. 3, 4, and 5) The first step along the degradation is hydrolysis of the ester bond yielding 4-hydroxybenzoic acid MP1 (MW = 138). The latter decarboxylates with a high barrier ( $53.8 \text{ kcal mol}^{-1}$ ) to produce MP2, which readily captures a  $\bullet\text{OH}$  at the *o*-/*p*- positions (MP6/MP7). MP7 reacts with another  $\bullet\text{OH}$  to yield either catechol (MP8) or hydroxyquinone (MP5). The degradation of MP5 and MP8 follow the same paths as those of SA5 and SA10.

**Fig. 5** Gibbs-free energies (kcal mol) for the degradation pathway of MP into MP5 and MP8 (B3LYP/6-31 + G\*, in water)



## Toxicity

The acute and chronic toxicity of the target compounds and their byproducts to aquatic organisms were predicted at three trophic levels (green algae, daphnia, and fish) and the results are presented in Table S1. The colors are based on reference toxicity classifications (Table S2) and used in assessing the harmfulness or safety of the target compounds and the

intermediate products. We found that SA is harmful to green algae and daphnia, and safe for fish, while MP is harmful to all three aquatic organisms. The results are consistent with the experimental findings reported in the literature (Clevers 2004). We also found that toxicity fluctuated between “harmful” and “toxic” as the reactions proceeded, and the byproducts SA14 and MP12 were more toxic than their parent molecules all three organisms. These are also consistent with



the literature reporting the experimental results to show higher toxicity of p-benzoquinone than phenolic parents (Degraeve et al. 1980). Note that quinones are Michael acceptors; damage due to these species sometimes result from covalent binding with cellular nucleophiles; it has also been demonstrated that some quinone molecules can react with nucleophilic amino groups on DNA or proteins (Bolton et al. 2000; Monks and Jones 2002).

The results presented in Table S1 show that, as the reactions proceed, the solution is detoxified, especially after the ring opening phase (SA15, SA16, SA17, SA18, MP13, MP14, MP15, and MP17). The values of EC<sub>50</sub> and LC<sub>50</sub> show that SA, MP, and their early oxidation byproducts are harmful, while the products formed later are not. The result is consistent with the literature reporting the reduction in the estrogenic activity of propylparaben upon degradation by AOPs, accompanied with an initial increase in the acute toxicity followed by a sharp decrease as the value of TOC decreases (Fang et al. 2013).

## Conclusions

This study has shown that the two common PPCPs, salicylic acid and methyl paraben, are readily oxidized by ultrasonic irradiation at 572 kHz to produce a variety of oxidation byproducts, which are partially mineralized within the allowed reaction time. Computational analysis of the reactions based on •OH-mediated oxidation, confirmed the formation of the experimentally identified byproducts SA3 (154), SA5 (110), SA8 (154), SA10 (110), SA14 (108), SA18 (62), MP1 (138), MP5 (110), MP8 (110), MP12 (108), MP15 (134), and MP17 (150), thus providing for the first time a detailed mechanistic account for the degradation of salicylic acid and methyl paraben.

ECOSAR toxicity analysis showed that SA is toxic to green algae and daphnid, but non-toxic to fish, while MP is “harmful” to all three levels of aquatic organisms. It was also found that the toxicity fluctuated between toxic-harmful-non-toxic levels during the degradation process. The most toxic byproduct was benzoquinone, which was formed upon the degradation of both compounds, and which is recognized as the most toxic derivative of benzene-bearing compounds.

Finally, the analysis of toxicity has shown that most of the oxidation byproducts are non-toxic to the test organisms, confirming the environmental friendliness of the applied AOP method, or showing sonochemistry as a powerful tool of green technology. Nevertheless, more research is required to establish the feasibility and sustainability of the method as a viable option to classical chemical methods of water treatment that consume high concentrations of chemicals and produce large volumes of hazardous sludge.

**Acknowledgments** The experimental part of the study was funded by Boğazici University Research Fund (BAP) through Project 18Y00D1.

## References

- Agopcan Cinar S, Ziylan-Yavaş A, Catak S, Ince NH, Aviyente V (2017) Hydroxyl radical-mediated degradation of diclofenac revisited: a computational approach to assessment of reaction mechanisms and by-products. *Environ Sci Pollut Res* 24:18458–18469. <https://doi.org/10.1007/s11356-017-9482-7>
- Amin A, Chauhan S, Dare M, Bansal AK (2010) Degradation of parabens by *Pseudomonas beteli* and *Burkholderia latens*. *Eur J Pharm Biopharm: Official Journal of Arbeitsgemeinschaft für Pharmazeutische Verfahrenstechnik* 75(2):206–212. <https://doi.org/10.1016/j.ejpb.2010.03.001>
- Becke AD (1993a) A new mixing of Hartree-Fock and local density-functional theories. *J Chem Phys* 98:1372–1377. <https://doi.org/10.1063/1.464304>
- Becke AD (1993b) Density-functional thermochemistry III. The role of exact exchange. *J Chem Phys* 98:5648–5652. <https://doi.org/10.1063/1.464913>
- Bolton JL, Trush MA, Penning TM, Dryhurst G, Monks TJ (2000) Role of quinones in toxicology. *Chem Res Toxicol* 13:135–160. <https://doi.org/10.1021/tx9902082>
- Brodin T, Fick J, Jonsson M, Klaminder J (2013) Dilute concentrations of a psychiatric drug alter behavior of fish from natural populations. *Science* (80-) 339:814–815. <https://doi.org/10.1126/science.1226850>
- Chang CY, Hsieh YH, Cheng KY, Hsieh LL, Cheng TC, Yao KS (2008) Effect of pH on Fenton process using estimation of hydroxyl radical with salicylic acid as trapping reagent. *Water Sci Technol* 58:873–879. <https://doi.org/10.2166/wst.2008.429>
- Chaniotakis NA, Park SB, Meyerhoff ME (1989) Salicylate-selective membrane electrode based on tin(IV) tetraphenylporphyrin. *Anal Chem* 61:566–570. <https://doi.org/10.1021/ac00181a013>
- Chatel G, Novikova L, Petit S (2016) How efficiently combine sonochemistry and clay science? *Appl Clay Sci* 119:193–201
- Cleuvers M (2004) Mixture toxicity of the anti-inflammatory drugs diclofenac, ibuprofen, naproxen, and acetylsalicylic acid. *Ecotoxicol Environ Saf* 59:309–315. [https://doi.org/10.1016/S0147-6513\(03\)00141-6](https://doi.org/10.1016/S0147-6513(03)00141-6)
- Degraeve GM, Geiger DL, Meyer JS, Bergman HL (1980) Acute and embryo-larval toxicity of phenolic compounds to aquatic biota. *Arch Environ Contam Toxicol* 568:557–568
- ECOSAR, (2014) <http://www.epa.gov/oppt/newchems/tools/21ecosar>.
- Fang H, Gao Y, Li G, An J, Wong PK, Fu H, Yao S, Nie X, An T (2013) Advanced oxidation kinetics and mechanism of preservative propylparaben degradation in aqueous suspension of TiO<sub>2</sub> and risk assessment of its degradation products. *Environ Sci Technol* 47:2704–2712. <https://doi.org/10.1021/es304898r>
- Frisch MJ, Trucks GW, Schlegel HB, et al (2009) Gaussian 09 Revision E.01. Gaussian 09, Revis. E.01
- Gao Y, Ji Y, Li G, An T (2016) Theoretical investigation on the kinetics and mechanisms of hydroxyl radical-induced transformation of parabens and its consequences for toxicity: influence of alkyl-chain length. *Water Res* 91:77–85. <https://doi.org/10.1016/j.watres.2015.12.056>
- George SJ, Gandhimathi R, Nidheesh PV, Ramesh ST (2014) Electro-Fenton oxidation of salicylic acid from aqueous solution: batch studies and degradation pathway. *Clean Soil Air Water* 42:1701–1711. <https://doi.org/10.1002/clen.201300453>
- Gmurek M, Rossi AF, Martins RC, Quinta-Ferreira RM, Ledakowicz S (2015) Photodegradation of single and mixture of parabens –

- kinetic, by-products identification and cost-efficiency analysis. *Chem Eng J* 276:303–314. <https://doi.org/10.1016/j.cej.2015.04.093>
- Guinea E, Arias C, Cabot PL, Garrido JA, Rodríguez RM, Centellas F, Brillas E (2008) Mineralization of salicylic acid in acidic aqueous medium by electrochemical advanced oxidation processes using platinum and boron-doped diamond as anode and cathodically generated hydrogen peroxide. *Water Res* 42:499–511. <https://doi.org/10.1016/j.watres.2007.07.046>
- Gültekin I, Ince NH (2007) Synthetic endocrine disruptors in the environment and water remediation by advanced oxidation processes. *J Environ Manag* 85:816–832. <https://doi.org/10.1016/j.jenvman.2007.07.020>
- Ince NH (2018), Ultrasound-assisted advanced oxidation processes for water decontamination. *Ultrason Sonochem* 40 (B):97–103. <https://doi.org/10.1016/j.ultsonch.2017.04.009>
- Karnik BS, Davies SH, Baumann MJ, Masten SJ (2007) Use of salicylic acid as a model compound to investigate hydroxyl radical reaction in an ozonation–membrane filtration hybrid process. *Environ Eng Sci* 24(6):852–860
- Lam SM, Sin JC, Zuhairi Abdullah A, Rahman Mohamed A (2013) Green hydrothermal synthesis of ZnO nanotubes for photocatalytic degradation of methylparaben. *Mater Lett* 93:423–426. <https://doi.org/10.1016/j.matlet.2012.12.008>
- Lee C, Hill C, Carolina N (1988) Role of massage in the management of an athlete. Pdf. 37. doi: <https://doi.org/10.1103/PhysRevB.37.785>
- Lin Y, Ferronato C, Deng N, Wu F, Chovelon JM (2009) Photocatalytic degradation of methylparaben by TiO<sub>2</sub>: multivariable experimental design and mechanism. *Appl Catal B Environ* 88:32–41. <https://doi.org/10.1016/j.apcatb.2008.09.026>
- Márquez-sillero I, Aguilera-herrador E, Cárdenas S, Valcárcel M (2010) Determination of parabens in cosmetic products using multi-walled carbon nanotubes as solid phase extraction sorbent and corona-charged aerosol detection system. *J Chromatogr A* 1217:1–6. <https://doi.org/10.1016/j.chroma.2009.11.005>
- Mason TJ, and Peters D. 2002. Practical sonochemistry: power ultrasound uses and applications. Woodhead Publishing. book
- Mason TJ, Lorimer JP, Bates DM (1992) Quantifying sonochemistry: casting some light on a black art. *Ultrasonics* 30(1):40–42
- Monks TJ, Jones DC (2002) The metabolism and toxicity of quinones, quinonimines, quinone methides, and quinone-thioethers. *Curr Drug Metab* 3:425–438. <https://doi.org/10.2174/1389200023337388>
- Nakada N, Shinohara H, Murata A, Kiri K, Managaki S, Sato N, Takada H (2007) Removal of selected pharmaceuticals and personal care products (PPCPs) and endocrine-disrupting chemicals (EDCs) during sand filtration and ozonation at a municipal sewage treatment plant. *Water Res* 41:4373–4382
- Ramaswamy BR, Kim JW, Isobe T, Chang KH, Amano A, Miller TW, Siringan FP, Tanabe S (2011) Determination of preservative and antimicrobial compounds in fish from Manila Bay, Philippines using ultra high performance liquid chromatography tandem mass spectrometry, and assessment of human dietary exposure. *J Hazard Mater* 192: 1739–1745. <https://doi.org/10.1016/j.jhazmat.2011.07.006>
- Sánchez-Martin J, Beltrán-Heredia J, Domínguez JR (2013) Advanced photochemical degradation of emerging pollutants: methylparaben. *Water Air Soil Pollut* 224:1483. <https://doi.org/10.1007/s11270-013-1483-7>
- Sasi S, Rayaroth MP, Devadasan D, Aravind UK, Aravindakumar CT (2015) Influence of inorganic ions and selected emerging contaminants on the degradation of methylparaben : a Sonochemical approach. *J Hazard Mater* 300:202–209. <https://doi.org/10.1016/j.jhazmat.2015.06.072>
- Savun-Hekimoğlu B, Ince NH (2017) Decomposition of PPCPs by ultrasound-assisted advanced Fenton reaction: a case study with salicylic acid. *Ultrason Sonochem* 39:243–249. <https://doi.org/10.1016/j.ultsonch.2017.04.013>
- Savun-Hekimoğlu B, Ince NH (2019) Sonochemical and sonocatalytic destruction of methylparaben using raw, modified and SDS-intercalated particles of a natural clay mineral. *Ultrason Sonochem* 54:233–240
- Scheck CK, Frimmel FH (1995) Degradation of phenol and salicylic acid by ultraviolet radiation/hydrogen peroxide/oxygen. *Water Res* 29: 2346–2352
- Suslick KS, Hammerton DA, Cline RE (1986) Sonochemical hot spot. *J Am Chem Soc* 108:5641–5642
- Tay KS, Rahman NA, Bin AMR (2010) Ozonation of parabens in aqueous solution: kinetics and mechanism of degradation. *Chemosphere* 81:1446–1453. <https://doi.org/10.1016/j.chemosphere.2010.09.004>
- Taylor P, Stamatis NK Personal care compounds and caffeine tracer in municipal sewage treatment plant in Western Greece. *J Environ Sci Health, Part B: Personal Care Compounds and Caffeine Tracer in Municipal Sewage Treatment Plant in Western Greece Occurrence and Removal of Emerging Pharmaceutical*, 37–41. <https://doi.org/10.1080/03601234.2013.781359>
- Wales S, Kasprzyk-hordern B, Dinsdale RM, Guwy AJ (2008) The occurrence of pharmaceuticals ,personal care products , endocrine disruptors and illicit drugs in surface water in. *Water Res* 42:3498–3518. <https://doi.org/10.1016/j.watres.2008.04.026>

**Publisher's note** Springer Nature remains neutral with regard to jurisdictional claims in published maps and institutional affiliations.